Bioconjugate Chemistry

Communication

pubs.acs.org/bc

^{18}F-Based Pretargeted PET Imaging Based on Bioorthogonal Diels–Alder Click Chemistry

Jan-Philip Meyer,[†] Jacob L. Houghton,[†] Paul Kozlowski,[†] Dalya Abdel-Atti,[†] Thomas Reiner,[†] Naga Vara Kishore Pillarsetty,[†] Wolfgang W. Scholz,[‡] Brian M. Zeglis,*[,§,∥] and Jason S. Lewis*[,†,⊥]

[†]Department of Radiology, Memorial Sloan Kettering Cancer Center, 1275 York Avenue, New York, New York 10065, United States

[‡]MabVax Therapeutics, 11588 Sorrento Valley Road Suite 20, San Diego, California 92121, United States

[§]Department of Chemistry, Hunter College of the City University of New York, 695 Park Avenue, New York, New York 10065, United States

[∥]The Graduate Center, City University of New York, 365 Fifth Avenue, New York, New York 10016, United States

[⊥]Molecular Pharmacology Program, Memorial Sloan Kettering Cancer Center, 1275 York Avenue, New York, New York 10065, United States

Supporting Information

ABSTRACT: A first-of-its-kind ^{18}F pretargeted PET imaging approach based on the bioorthogonal inverse electron demand Diels–Alder (IEDDA) reaction between tetrazine (Tz) and trans-cyclooctene (TCO) is presented. As proof-of-principle, a TCO-bearing immunoconjugate of the anti-CA19.9 antibody 5B1 and an Al[^{18}F]NOTA-labeled tetrazine radioligand were harnessed for the visualization of CA19.9-expressing BxPC3 pancreatic cancer xenografts. Biodistribution and ^{18}F-PET imaging data clearly demonstrate that this methodology effectively delineates tumor mass with activity concentrations up to 6.4 %ID/g at 4 h after injection of the radioligand.

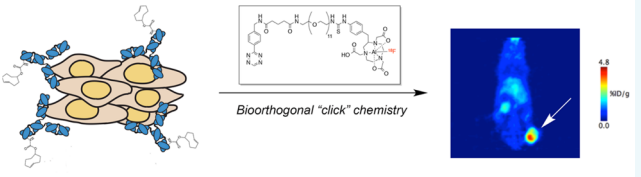

Over the past two decades, pretargeting strategies linking antibody targeting vectors and small molecule radioligands have emerged as powerful tools for the in vivo positron emission tomography (PET) of cancer.[1] These methods effectively leverage the principal advantages of both species while skirting their inherent limitations.[2] Despite their slow pharmacokinetics, antibodies possess remarkable specificity and affinity for tumor biomarkers, and thus immunoconjugates bearing click chemistry moieties can provide excellent targeted platforms for in vivo bioorthogonal reactions.[3] In most pretargeting methodologies, the in vivo hapten is a radiolabeled small molecule with rapid pharmacokinetics. Without question, the most important facet of pretargeting strategies is the ability to radiolabel the antibody after it has reached the tumor, a trait which facilitates the use of short-lived radioisotopes that would normally be incompatible with the multiday biological half-lives of IgG vectors. This, in turn, dramatically reduces the radiation doses to healthy tissues compared to traditional radioimmunoconjugates directly labeled with long-lived radioisotopes such as ^{124}I ($t_{1/2}$ = 4.2 d) or ^{89}Zr ($t_{1/2}$ = 3.2 d).[4]

The IEDDA reaction between a 1,2,4,5-tetrazine (Tz) and a trans-cyclooctene (TCO) is one of the most rapid bioorthogonal click ligations and, as such, is remarkably well suited for pretargeting strategies.[5−9] Indeed, pretargeted imaging based on the IEDDA reaction has already been proven to be feasible in vivo.[3,6−10] For example, the human A33 (huA33) antibody and a ^{64}Cu-labeled radioligand have recently been successfully employed for the pretargeted PET imaging of SW1222 human colorectal cancer xenografts.[3,11] In this case, it was shown that the pretargeted approach visualized the malignant tissue with comparable tumor-to-background contrast at only a fraction of the off-target radiation dose to healthy tissue, when compared to traditional radioimmunoconjugation approaches.

With this in mind, it follows that the creation of a pretargeting strategy featuring an even shorter-lived radionuclide such as ^{18}F ($t_{1/2}$ = 109.8 min) is the next logical step, as this could exploit the dosimetric advantages of pretargeting even further. The aluminum-[^{18}F]fluoride-NOTA-complex[12−14] (Al[^{18}F]-NOTA) has previously been shown to be a stable and synthetically efficient methodology for the radiolabeling of both biomolecules[15,16] and small molecules[17] with [^{18}F]fluoride. Considering the well-documented instability of tetrazines under the alkaline conditions required for nucleophilic ^{18}F-fluorination reactions, the Al[^{18}F]-NOTA approach seems to be particularly appropriate for the synthesis of ^{18}F-labeled tetrazine radioligands.[18−20] Despite known procedures for the radiosynthesis of ^{18}F-labeled TCO,[21,22] we chose to apply the Al[^{18}F]-NOTA-approach to tetrazines in

Special Issue: Molecular Imaging Probe Chemistry

Received: September 16, 2015
Revised: October 16, 2015
Published: October 19, 2015

DOI: 10.1021/acs.bioconjchem.5b00504
Bioconjugate Chem. 2016, 27, 298−301

order to be able to use readily available TCO-modified 5B1 for in vivo pretargeting of CA19.9.

Herein, we report the development of a novel Tz/TCO-based pretargeting strategy using an Al[^{18}F]-NOTA-labeled tetrazine radioligand. For our proof-of-concept system, we selected the 5B1 antibody, a fully human IgG that targets a promising biomarker for pancreatic ductal adenocarcinoma: carbohydrate antigen 19.9 (CA19.9).[23,24] In order to arm the antibody with the reactive bioorthogonal moiety, purified 5B1 was incubated with an activated succinimidyl ester of TCO (TCO-NHS, 35 equiv.) at room temperature for 1 h. The immunoconjugate was subsequently purified by gel-filtration chromatography. The precursor to the radioligand, Tz-PEG$_{11}$-NOTA (**1**, Scheme 1), was synthesized from three

Scheme 1. Radiochemical Synthesis of the Radioligand Tz-PEG$_{11}$-Al[^{18}F]-NOTA ([^{18}F]2)[a]

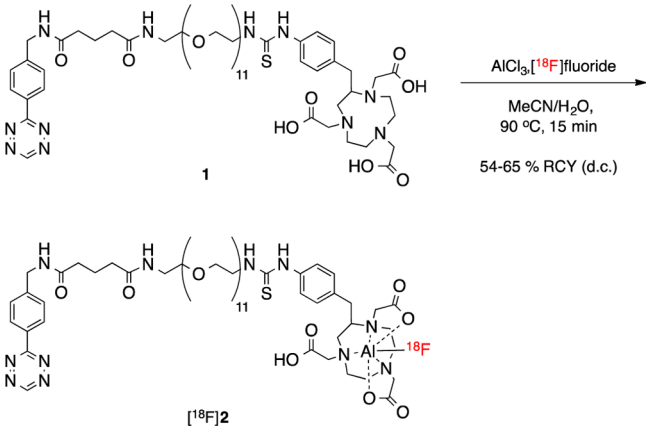

[a] [^{18}F]**2** was obtained in 54−56% RCY (d.c.) and high SAs (21.4−26.7 GBq/μmol) after a total synthesis time of 108 min. Purification of the crude reaction mixture using a C18-cartridge gave [^{18}F]**2** in purities >96%.

commercially available building blocks: 2,5-dioxo-1-pyrrolidinyl 5-[4-(1,2,4,5-tetrazin-3-yl)benzylamino]-5-oxopentanoate (Tz-NHS), *O*-(2-aminoethyl)-*O*′-[2-(boc-amino)ethyl]-decaethylene glycol (NH$_2$-PEG$_{11}$-NHBoc), and *S*-2-(4-isothiocyanatobenzyl)-1,4,7-triaza-cyclononane-1,4,7-triacetic acid (*p*-SCN-Bn-NOTA). After the peptide coupling between Tz-NHS and NH$_2$-PEG$_{11}$-NHBoc and the subsequent deprotection of the terminal *tert*-butyloxycarbonyl protecting group, the resulting Tz-PEG$_{11}$-NH$_2$ moiety was reacted with the bifunctional *p*-SCN-Bn-NOTA chelator. Ultimately, the precursor was prepared in very high purity (>98%) and with an overall yield of ∼15% (n = 3).

The ^{18}F-labeled radioligand Tz-PEG$_{11}$-Al[^{18}F]-NOTA ([^{18}F]**2**) was obtained in 54−65% radiochemical yield [decay-corrected (d.c.) to the start of synthesis] in high purity (>96%) and a specific activity between 21.4 and 26.7 GBq/μmol (for more detailed experimental data, see Supporting Information). The use of metal-free solvents, the pH of the Al[^{18}F]-NOTA complexation reaction (pH = 4), and the ratio of reaction solvents (at least 3:1 MeCN/H$_2$O) all proved to be crucial factors in obtaining high radiochemical yields. The in vitro stability of [^{18}F]**2** was assayed by incubation in phosphate buffered saline (PBS, pH 7.4) or human serum at 37 °C, followed by analysis via radio-HPLC. In PBS, negligible decomposition could be observed after 4 h (92 ± 2.3% intact), and 79 ± 4.4% (n = 4) of the radioligand remained intact in human serum at the same time point. The in vivo stability was determined by injecting [^{18}F]**2** (150 μCi in 150 μL 0.9% sterile saline) into healthy athymic nude mice. Blood was subsequently collected via cardiac puncture and 63 ± 8.9% (n = 3) of the radioligand was found intact 4 h after injection. Given the fast reaction kinetics of the IEDDA ligation as well as the relatively short half-life of ^{18}F, the observed degradation rate is not considered a detriment to the system, as shown for other Tz/TCO approaches.[3,19]

The bioorthogonal click reaction between [^{18}F]**2** and the TCO moiety on the antibody was demonstrated by incubation of equimolar amounts (1.33 nmol) of the purified radioligand with 5B1-TCO at room temperature. Analysis of the reaction via radio-TLC (mobile phase: 90% MeCN in H$_2$O) revealed a > 94% yield for the reaction measured by the consumption of [^{18}F]**2**, with the ^{18}F-labeled click reaction product situated at the origin, while the free radioligand can be detected at the solvent front (see Supporting Information). In all experiments throughout this study, the equimolar amount of tetrazine is calculated relative to the antibody 5B1 (and not the TCO).

Ex vivo biodistribution data for Tz-PEG11-Al[^{18}F]-NOTA were first obtained in healthy mice by injecting [^{18}F]**2** alone (1.8−2.0 MBq) via the tail vein (Figure 1). The data shows

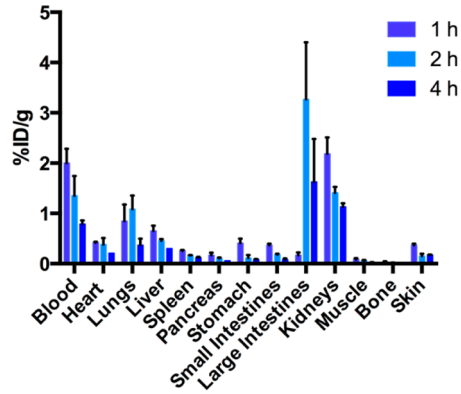

Figure 1. Biodistribution of the radioligand [^{18}F]**2** in healthy athymic nude mice. The ^{18}F-labeled tracer (1.33 nmol, 1.8−2.0 MBq) was injected via the tail vein before the mice were euthanized, and the organs collected at the appropriate time points.

accumulation and retention of the radiotracer in the large intestines and feces with 0.32 ± 0.87% injected dose per gram (%ID/g) at 1 h after injection to 1.73 ± 0.45 %ID/g at 4 h. The uptake and retention of [^{18}F]**2** could also be observed in the kidneys (2.12 ± 0.23 %ID/g at 1 h to 1.17 ± 0.12% ID/g at 4 h), indicating dual renal and fecal elimination pathways for the radioligand. The amount of activity in the blood decreases over time, from 1.94 ± 0.23 %ID/g at 1 h to 0.78 ± 0.08 %ID/g at 4 h after injection, while the uptake in all other healthy tissues remained <1 %ID/g. Critically, the activity concentrations in the bone were particularly low (≤0.2 %ID/g), illustrating the high in vivo stability of the Al[^{18}F]-NOTA complex. In accompanying experiments, the blood half-life of the radioligand was calculated to be 71.2 ± 5.4 min.

In subsequent pretargeted biodistribution experiments, nude, athymic mice bearing subcutaneous CA19.9-expressing BxPC3 xenografts were injected with 5B1-TCO (1.33 nmol of 5B1) 72 h prior to the administration of [^{18}F]**2** (1.33 nmol, 1.8−2.0 MBq) (Figure 2).

DOI: 10.1021/acs.bioconjchem.5b00504
Bioconjugate Chem. 2016, 27, 298−301

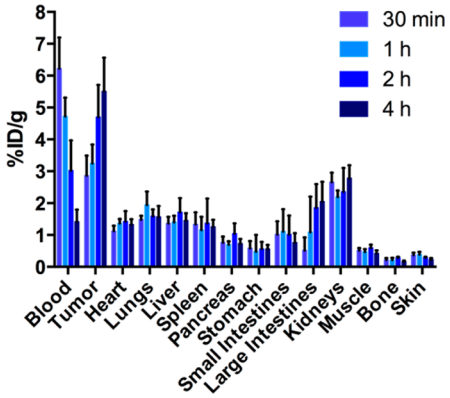

Figure 2. Results of the biodistribution pretargeting CA19.9 with [^{18}F]**2**/5B1-TCO. Subcutaneous BxPC3 xenograft bearing mice were administered 5B1-TCO (1.33 nmol) 72 h prior to the injection of the ^{18}F-labeled tracer (1.33 nmol, 1.8−2.0 MBq) via the tail vein before the mice were euthanized, and the organs collected at the appropriate time points.

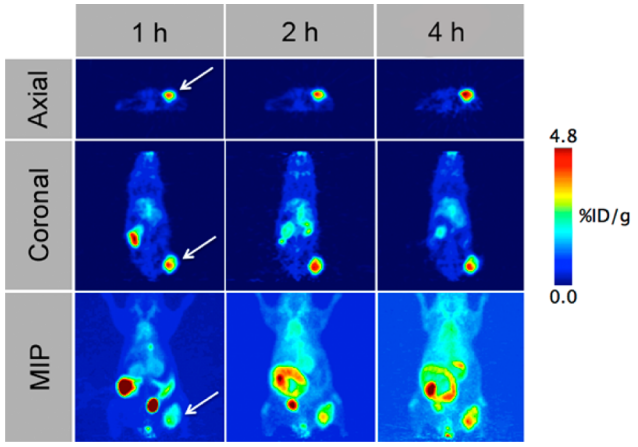

Figure 3. PET images of Tz-PEG$_{11}$-Al[^{18}F]-NOTA/5B1-TCO pretargeting strategy. Subcutaneous BxPC3 xenograft bearing mice were administered 5B1-TCO (1.33 nmol) 72 h prior to the injection of the ^{18}F-labeled tracer (1.33 nmol, 18−20 MBq) via the tail vein. Transverse (top) and coronal (middle) planar images intersect the center of the tumors. The maximum intensity projections (MIPs, bottom) clearly illustrate tumor uptake after 1 h with increasing tumor-to-background ratios over the course of the experiment.

The data revealed increasing tumoral uptake over the course of the study (3.0 ± 0.32 %ID/g at 30 min, 3.52 ± 0.67 %ID/g at 1 h, 4.81 ± 1.23 %ID/g at 2 h to 5.6 ± 0.85 %ID/g at 4 h), with the amount of radioactivity in the blood decreasing in kind, from 6.13 ± 0.86 %ID/g at 30 min to 1.75 ± 0.22 %ID/g at 4 h. In accordance with the biodistribution data obtained from healthy mice, the uptake in other tissue remained generally low (≤2 %ID/g), with the highest uptake and retention in the clearance organs: the intestines and kidneys. The clearance of radioactivity from the blood pool was generally in line with the calculated blood half-life of the radiotracer, and the steady uptake of radioactivity at the tumor suggested that the radioligand is primarily clicking with 5B1-TCO at the tumor site rather than clicking in the blood pool followed by accumulation at the tumor.

Pretargeted small animal PET imaging experiments were conducted in a similar fashion, with the only difference in the amount of radioactivity injected (18−20 MBq, 1.33 nmol of [^{18}F]**2**, equimolar to 5B1-TCO) (Figure 3).

The PET images confirm the data obtained in the biodistribution study: the signal in the tumor increases with time, while the activity concentrations in the blood and intestines concomitantly decrease. This results in the clear delineation of the tumor from background tissue, with the tumor-to-background activity ratios improving over the course of the experiment. The tumoral uptake of [^{18}F]**2** is immediately evident 1 h after injection; however, the signal grows to 6.4 %ID/g at 4 h after the administration of the radioligand. Admittedly, while the tumor-to-background activity concentration ratios improve over time, the radioactivity has not cleared the intestines at 4 h postinjection. Considering the blood half-life (71.2 ± 5.4 min) of the radioligand and the observed increasing tumor uptake over the course of the experiment, it seems reasonable and interesting to include a later imaging and biodistribution time point (e.g., 6 h p.i.) in future experiments in order to evaluate whether an improved tumor-to-background ratio can be observed at later time points. In terms of control conditions, previous studies in our laboratory have shown that no tumor uptake could be observed when IgG-TCO instead of 5B1-TCO was injected into BxPC3-bearing mice, suggesting that the observed tumor uptake is a result of in vivo click reactions occurring at the tumor site.[3,25]

In light of these results, second generation tetrazine-bearing radioligands are currently in development in our laboratory in an effort to determine whether structural alterations can increase the fraction of the radioligand that is excreted via the renal system and thus create higher tumor-to-background ratios at earlier time points. Finally, using the biodistribution data, we performed a dosimetric analysis of the pretargeting strategy that confirms that pretargeted PET imaging with Tz-PEG$_{11}$-Al[^{18}F]-NOTA and 5B1-TCO confers a significant dosimetric advantage over the use of antibodies directly labeled with long-lived radioisotopes (in this case ^{89}Zr-DFO-5B1). The effective dose of the presented ^{18}F-based pretargeting system (0.03 rem/mCi) is more than 60 times lower than directly labeled ^{89}Zr-DFO-5B1 (2.02 rem/mCi; see Supporting Information).

In sum, this novel ^{18}F-based pretargeted PET imaging system shows highly promising biodistribution results and produced tumoral activity concentrations of up to 6.4 %ID/g at 4 h postinjection. Small-animal PET imaging experiments revealed that this methodology clearly delineates CA19.9-expressing tissues with especially enticing tumor-to-background activity ratios 2 and 4 h after injection of the radiotracer.

■ ASSOCIATED CONTENT

Supporting Information

The Supporting Information is available free of charge on the ACS Publications website at DOI: 10.1021/acs.bioconjchem.5b00504.

Synthesis of the precursor **1**, dosimetry calculations, and experimental details (PDF)

■ AUTHOR INFORMATION

Corresponding Authors

*E-mail: Lewisj2@mskcc.org.
*E-mail: brian.zeglis@hunter.cuny.edu.

DOI: 10.1021/acs.bioconjchem.5b00504
Bioconjugate Chem. 2016, 27, 298−301

Notes

The authors declare the following competing financial interest(s): Wolfgang W. Scholz is an employee of MabVax Therapeutics and has an equity interest.

■ ACKNOWLEDGMENTS

The authors gratefully acknowledge the MSKCC Small Animal Imaging Core Facility as well as the Radiochemistry and Molecular Imaging Probe core, which were supported in part by NIH grant P30 CA08748. The authors also would like to thank the NIH (K25 EB016673, T.R.; F32 CA180452 and R25CA096945, J.L.H.; 4R00 CA178205-2, B.M.Z.; 2R42CA128362, MabVax). We also gratefully acknowledge Mr. William H. and Mrs. Alice Goodwin and the Commonwealth Foundation for Cancer Research and The Center for Experimental Therapeutics of Memorial Sloan Kettering Cancer Center.

■ REFERENCES

(1) Rossin, R., and Robillard, M. S. (2014) Pretargeted imaging using bioorthogonal chemistry in mice. *Curr. Opin. Chem. Biol. 21*, 161−9.

(2) Goldenberg, D. M., Sharkey, R. M., Paganelli, G., Barbet, J., and Chatal, J. F. (2006) Antibody pretargeting advances cancer radioimmmunodetection and radioimmunotherapy. *J. Clin. Oncol. 24*, 823−34.

(3) Zeglis, B. M., Sevak, K. K., Reiner, T., Mohindra, P., Carlin, S. D., Zanzonico, P., Weissleder, R., and Lewis, J. S. (2013) A pretargeted PET imaging strategy based on bioorthogonal Diels-Alder click chemistry. *J. Nucl. Med. 54*, 1389−96.

(4) Zhu, J., Li, S., Waengler, C., Waengler, B., Lennox, R. B., and Schirmmacher, R. (2015) Synthesis of 3-chloro-6-((4-(di-tert-butyl-[18F]-fluorosilyl)-benzyl)oxy)-1,2,4,5-tetrazine ([18F]SiFA-OTz) for rapid tetrazine-based ^{18}F-radiolabeling. *Chem. Commun. 51*, 12415−18.

(5) Goldenberg, D. M., Chang, C., Rossi, E. A., McBride, W. J., and Sharkey, R. M. (2012) Pretargeted Molecular Imaging and Radioimmunotherapy. *Theranostics 2*, 523−40.

(6) Van deWatering, F. C. J., Rijpkema, M., Robillard, M., Oyen, W. J. G., and Boerman, O. C. (2014) Pretargeted Imaging and Radioimmunotherapy of cancer using antibodies and bioorthogonal chemistry. *Front. Med. 1*, 1−11.

(7) Devaraj, N. K., and Weissleder, R. (2011) Biomedical Applications of tetrazine Cycloadditions. *Acc. Chem. Res. 44*, 816−27.

(8) Emmetiere, F., Irwin, C., Viola-Villegas, N. T., Longo, V., Cheal, S. M., Zanzonico, P., Pillarsetty, N., Weber, W. A., Lewis, J. S., and Reiner, T. (2013) ^{18}F-Labeled-Bioorthogonal Liposomes for *In Vivo* Targeting. *Bioconjugate Chem. 24*, 1784−89.

(9) Denk, C., Svatunek, D., Filip, T., Wanek, T., Lumpi, D., Froehlich, J., Kuntner, C., and Mikula, H. (2014) Development of a ^{18}F-labeled tetrazine with favorable pharmacokinetics for bioorthogonal PET imaging. *Angew. Chem., Int. Ed. 53*, 9655−59.

(10) Herth, M. M., Andersen, V. L., Lehel, S., Madsen, J., Knudsen, G. M., and Kristensen, J. L. (2013) Development of a ^{11}C-labeled tetrazine for rapidtetrazine-trans-cyclooctene ligation. *Chem. Commun. 49*, 3805−7.

(11) Zeglis, B. Z., Brand, C., Abdel-Atti, D., Carnazza, K. E., Cook, B. E., Carlin, S., Reiner, T., and Lewis, J. S. (2015) Optimization of a Pretargeted Strategy for the PET Imaging of Colorectal Carcinoma via the Modulation of Radioligand Pharmacokinetics. *Mol. Pharmaceutics 12*, 3575−87.

(12) McBride, W. J., D'Souza, C. A., Sharkey, R. M., Karacay, H., Chang, C., and Goldenberg, D. M. (2010) Improved ^{18}F Labeling of Peptides with a Fluoride-Aluminum Chelate Complex. *Bioconjugate Chem. 21*, 1331−40.

(13) Richter, S., and Wuest, F. (2014) ^{18}F-Labeled Peptides: The Future Is Bright. *Molecules 19*, 20536−56.

(14) Pan, D., Yan, Y., Yang, R., Xu, Y. P., Chen, F., Wang, L., Luo, S., and Yang, M. (2014) PET imaging of prostate tumors with ^{18}F-Al-NOTA-MATBBN. *Contrast Media Mol. Imaging 9*, 342−8.

(15) McBride, W. J., Sharkey, R. M., Karacay, H., D'Souza, C. A., Rossi, E. A., Laverman, P., Chang, C., Boerman, O. C., and Goldenberg, D. M. (2009) A novel method for ^{18}F Radiolabeling for PET. *J. Nucl. Med. 50*, 991−8.

(16) McBride, W. J., D'Souza, C. A., Karacay, H., Sharkey, R. M., and Goldenberg, D. M. (2012) New Lyophilized Kit for Rapid Radiofluorination of Peptides. *Bioconjugate Chem. 23*, 538−47.

(17) Hoigebazar, L., Jeong, J. M., Lee, J., Shetty, D., Yang, B. Y., Lee, Y., Lee, D. S., Chung, J., and Lee, M. C. (2012) Syntheses of 2-Nitroimidazole Derivatives Conjugated with 1,4,7-Tiazacyclononae-N,N′-Diacetic Acid Labeled with F-18 Using an Aluminum Complex Method for Hypoxia Imaging. *J. Med. Chem. 55*, 3155−62.

(18) Zeglis, B. M., Emmetiere, F., Pillarsetty, N., Weissleder, R., Lewis, J. S., and Reiner, T. (2014) Building Blocks for the Construction of Bioorthogonally Reactive Peptides via Solid Phase Peptide Synthesis. *ChemistryOpen 3*, 48−53.

(19) Karver, M. R., Weissleder, R., and Hilderbrand, S. A. (2011) Synthesis and evaluation of a series of 1,2,4,5-tetrazines for bioorthogonal conjugation. *Bioconjugate Chem. 22*, 2263−70.

(20) Reiner, T., and Zeglis, B. M. (2014) The inverse electron demand Diels-Alder click reaction in radiochemistry. *J. Labelled Compd. Radiopharm. 57*, 285−90.

(21) Jacobson, O., Kiesewetter, D. O., and Chen, X. (2015) Fluorine-18 Radiochemistry − Labeling Strategies and Synthetic Routes. *Bioconjugate Chem. 26*, 1−18.

(22) Wyffels, L., Thomae, D., Waldron, A., Fissers, J., Dedeurwaerdere, S., Van den Veken, P., Joossens, J., Stroobants, K., Augustyns, K., and Staelens, S. (2014) In vivo evaluation of ^{18}F-labeled TCO for pre-targeted PET imaging in the brain. *Nucl. Med. Biol. 41*, 513−523.

(23) Viola-Villegas, N. T., Rice, S. L., Carlin, S., Wu, X., Evans, M. J., Sevak, K. K., Drobjnak, M., Ragupathi, G., Sawada, R., Scholz, et al. (2013) Applying PET to broaden the diagnostic utility of the clinically validated CA19.9 serum biomarker for oncology. *J. Nucl. Med. 54*, 1876−1882.

(24) Chan, A., Prassas, I., Dimitromanolakis, A., Brand, R. E., Serra, S., Diamandis, E. P., and Blasutig, I. M. (2014) Validation of Biomarkers that complement CA19.9 in Detecting Early Pancreatic Cancer. *Clin. Cancer Res. 20*, 5787−95.

(25) Houghton, J. L., Zeglis, B. M., Abdel-Atti, D., Sawada, R., Scholz, W. W., and Lewis, J. S. (2015) Pretargeted immunoPET imaging of CA19.9: overcoming circulating antigen and internalized targeting vector to reduce radiation doses. *J. Nucl. Med.* [Online early access]. DOI: 10.2967/jnumed.115.163824. Published Online: Oct 15, 2015. http://jnm.snmjournals.org/content/early/2015/10/14/jnumed.115.163824.long (accessed Oct 15, 2015).

DOI: 10.1021/acs.bioconjchem.5b00504
Bioconjugate Chem. 2016, 27, 298−301